FULL PAPER

Luminescent platinum(IV) complexes bearing cyclometalated 1,2,3-triazolylidene and bi- or terdentate 2,6-diarylpyridine ligands

Ángela Vivancos,[a] Delia Bautista[b] and Pablo González-Herrero*[a]

Abstract: The synthesis, structure and photophysical properties of luminescent Pt^{IV} complexes that combine cyclometalated 1,2,3-triazolylidene and bi- or terdentate 2,6-diarylpyridine ligands are reported. The targeted complexes represent the first examples of Pt^{IV} species with a cyclometalated mesoionic aryl-NHC ligand. They exhibit moderate or weak emissions in fluid solution at 298 K arising from ^{3}LC states, which becomes very intense in PMMA matrices at 298 K. DFT and TD-DFT calculations confirm that the chromophoric ligand is the cyclometalated 2,6-diarylpyridine and show that the aryl-NHC ligand exerts a beneficial effect on the emission efficiencies of these derivatives by increasing the energy of deactivating LMCT excited states with respect to comparable Pt^{IV} complexes with cyclometalated 2-arylpyridines.

Introduction

Transition-metal complexes that exhibit long-lived and highly efficient luminescence remain the focus of intense study because of their use in a variety of photochemical, photobiological, biomedical, and optoelectronic applications, including chemical and biological sensing,[1–3] cell imaging,[4–7] photocatalysis in organic synthesis,[8,9] photodynamic therapy,[10,11] and electroluminescent materials for lighting and displays.[12–15] Complexes of Ir^{III}[16,17] and Pt^{II}[18,19] with cyclometalating heteroaromatic ligands have concentrated the majority of research efforts in this field during the most recent decades because of the high versatility of their excited states, whereas complexes of Au^{III} are being increasingly studied.[20,21] In comparison, cyclometalated Pt^{IV} complexes are very scarce and the study of their photophysical properties is still underdeveloped. The reported cyclometalated Pt^{IV} complexes for which luminescence studies have been carried out contain ligands of the 2-arylpyridine type (C^N) and are limited to a few types: (1) bis-cyclometalated complexes with a C_2-symmetrical $Pt(C^N_2)_2$ unit, $[Pt(C^N)_2(N^N)]^{2+}$ (N^N = aromatic diimine)[22] or $[Pt(C^N)_2X_2]$ (X = halide or carboxylate),[23,24] (2) bis-cyclometalated complexes with an unsymmetrical $Pt(C^N_2)_2$ unit, $[Pt(C^N)_2X_2]$[23] or $[Pt(C^N)_2(R)(X)]$ (R = alkyl[25,26] or C_6F_5[27]), and (3) meridional and (4) facial isomers of tris-cyclometalated complexes, *mer/fac*-$[Pt(C^N)_3]^+$.[28–30]

Pt^{IV} complexes with cyclometalating 2-arylpyridines emit from ligand-centered triplet excited states (^{3}LC) with very little metal-to-ligand charge-transfer (MLCT) character mixed in. Their emissions are typically characterized by very long lifetimes (from tens to hundreds of microseconds) and can reach very high quantum yields (up to 0.81) in fluid solution,[25,28] which could make them suitable for applications in the fields of chemosensing, cell imaging or photocatalysis. In comparison with related Ir^{III} or Pt^{II} complexes, the MLCT contribution to the emitting state is greatly diminished because of the very low energy of the occupied d orbitals in Pt^{IV}, but it plays a crucial role in the emissive behaviour of these complexes because it translates into an effective intersystem crossing through a spin–orbit coupling (SOC) mechanism, which facilitates the formation of the emitting triplet state and the radiative transition to the singlet ground state. In fact, recent results from our research group have demonstrated that variations in the degree of MLCT admixture into the emitting state are possible and have a decisive influence on the radiative rate constants (k_r) and emission efficiencies of cyclometalated Pt^{IV} complexes. Thus, uncharged derivatives often exhibit higher k_r values than cationic ones, due to a higher metal orbital involvement in the highest occupied molecular orbitals and hence a higher MLCT contribution to the emitting state.[23,25] Increased MLCT admixtures are also found for complexes with shorter Pt–C bonds from the cyclometalating ligands and/or containing suitable π-donor ancillary ligands, such as the fluoride ion, which result in higher energies of the occupied dπ orbitals.[23]

A second key factor affecting the emission efficiencies of cyclometalated Pt^{IV} complexes is the existence and/or energy of thermally accessible excited states of ligand-to-metal charge-transfer (LMCT) character resulting from electronic transitions to dσ* orbitals, which may provide nonradiative deactivation pathways. Higher energies of LMCT states correlate with lower nonradiative rate constants (k_{nr}) and higher emission efficiencies, and are attained for complexes containing shorter Pt–C bonds and/or an increased number of these bonds, which have a strong σ-donating character and lead to larger ligand-field splittings and higher dσ* orbital energies.[23,25]

In the present study, we have addressed the development of luminescent complexes that combine a mono- or di-cyclometalated 2,6-diarylpyridine (C^N^CH or C^N^C, respectively) and a cyclometalated mesoionic aryl-*N*-heterocyclic carbene (aryl-NHC) ligand (C^C*) in the coordination sphere of Pt^{IV}, aimed at attaining an increased number of Pt–C bonds with respect to the previously reported Pt^{IV} emitters. We note that the use of tridentate C^N^C ligands has most often led to weakly or non-emissive complexes with the Pt^{II} ion due to geometrical distortions in the triplet excited state,[31] with the remarkable exceptions of the strongly emissive complexes with *o*-carborane-

[a] *Dr. Á. Vivancos, Dr. P. González-Herrero*
Departamento de Química Inorgánica, Facultad de Química
Universidad de Murcia, Apdo. 4021, 30071 Murcia (Spain)
E-mail: pgh@um.es

[b] *Dr. D. Bautista*
SAI, Universidad de Murcia, Apdo. 4021, 30071 Murcia (Spain)

Supporting information for this article is given via a link at the end of the document.

substituted[32] or π-extended[33] C^N^C ligands, but significantly emissive complexes bearing this class of ligands have been obtained with the more electrophilic Ir^{III}[34] or Au^{III}[35–41] ions. The chosen aryl-NHC ligand belongs to the 1,2,3-triazolylidene subclass, presenting a reduced heteroatom stabilization and stronger σ-donating ability as compared to normal Arduengo-type NHCs.[42,43] We anticipated that the donor properties of the triazolylidene moiety would benefit the emission efficiencies of cyclometalated Pt^{IV} complexes by increasing the energy of deactivating excited states of LMCT character in a greater extent than do 2-arylpyridines. Cyclometalating aryl-NHC ligands have been previously employed for the synthesis of luminescent complexes of Ir^{III},[44–52] Pt^{II}[53–56] or Au^{III}[57] with enhanced emission properties, often as non-chromophoric, supporting ligands. However, most of them are normal 2-imidazolylidene-type aryl-NHCs, while mesoionic aryl-NHCs have been only employed to prepare a limited number of luminescent Pt^{II} complexes of the type [Pt(C^C*)(O^O)] (O^O = β-diketonate).[58,59] To the best of our knowledge, Pt^{IV} species bearing this class of ligand have not been reported to date.

Results and Discussion

Synthesis

The complexes $[Pt_2(\mu\text{-}Cl)_2(dtpyH)_2]$ (**1**) and [Pt(dtpy)(DMSO)] (**2**), containing mono- or dicyclometalated 2,6-di(*p*-tolyl)pyridine (dtpyH or dtpy, respectively), were synthesized following the procedures described for the analogous 2,6-diphenylpyridine complexes[60] and employed as starting materials. The introduction of the aryl-NHC ligand was then attempted via transmetalation from the silver carbene intermediate "AgI(trzH)" (trzH = 4-butyl-3-methyl-1-phenyl-1*H*-1,2,3-triazol-5-ylidene), which can be generated by reacting the triazolium salt with Ag_2O and used in situ.[42,43] The reaction of the dichloro-bridged dimer **1** with "AgI(trzH)" in 1:2 molar ratio led to the selective formation of *trans-C,C**-[PtCl(dtpyH)(trzH)] (*trans-C,C**-**3**; 91%), in which the triazolylidene ligand coordinates in *trans* to the metalated tolyl group (Scheme 1). The exclusive formation of this isomer is likely a consequence of the higher kinetic lability of the Pt–Cl bond in trans to the metalated tolyl group in **1**, as compared to that in trans to the pyridine moiety.

The ligand arrangement in *trans-C,C**-**3** is similar to that in complexes of the type [PtMe(C^N)(N^CH)], which we have shown to undergo the photochemical cyclometalation of the coordinated N^CH ligand upon irradiation with visible light to give bis-cyclometalated complexes *cis*-$[Pt(C^N)_2]$ and methane.[61] Based on this precedent, we attempted the cyclometalation of the coordinated trzH ligand in complex *trans-C,C**-**3** by irradiating an acetone solution of the complex with visible light (blue LEDs) in the presence of a base. However, this reaction led to the formation of [Pt(dtpy)(trzH)] (**4**; 69%), resulting from the metalation of the second *p*-tolyl group of the dtpyH ligand, which must be preceded by an isomerization to *cis-C,C**-**3**. In fact, when an acetone solution of complex *trans-C,C**-**3** is exposed to blue LEDs in the absence of base, complex *cis-C,C**-**3** is obtained (60%), demonstrating that the isomerization step is photochemical. Upon treatment of *cis-C,C**-**3** with base in acetone at room temperature, the cyclometalation step takes place to give **4**, confirming that this second step does not require light. Complex **4** could also be obtained directly by reacting the precursor [Pt(dtpy)(DMSO)] (**2**) with "AgI(trzH)" (87%), as has been reported for related species containing 2-imidazolylidene ligands.[62]

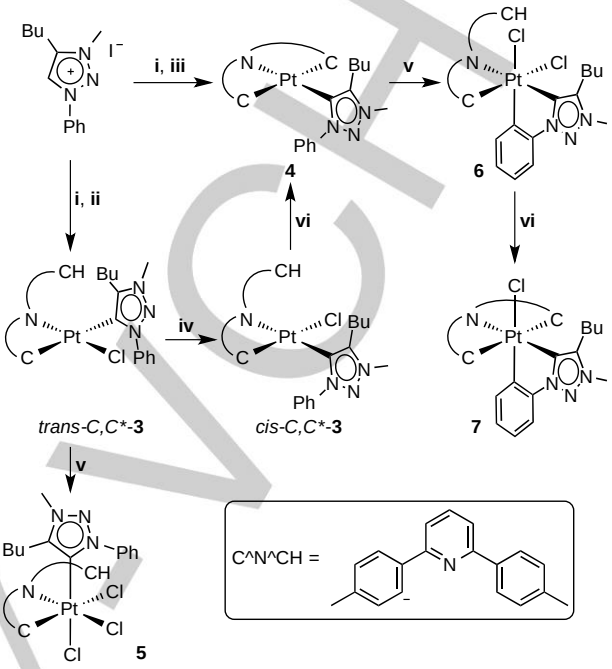

Scheme 1. Synthetic routes to the new complexes. i) Ag_2O; ii) $[Pt_2(\mu\text{-}Cl)_2(dtpyH)_2]$ (**1**); iii) [Pt(dtpy)(DMSO)] (**2**); iv) blue LEDs; v) $PhICl_2$; vi) base (AcONa or Na_2CO_3).

The isomerization of complex *trans-C,C**-**3** to *cis-C,C**-**3** is clearly evidenced in the ^1H NMR spectra by the resonance of the proton in ortho to the metalated carbon of the dtpyH ligand, which appears as a singlet with ^{195}Pt satellites at 7.84 ppm for the trans isomer, while it is significantly upfield-shifted to 6.21 ppm for the cis isomer, because in this isomer it is located over the shielding region produced by the diamagnetic current of the triazolylidene ring. The dicyclometalation of the dtpy ligand in complex **4** is confirmed by its ^1H NMR spectrum, which shows only one set of signals for the equivalent tolyl groups and a 6H singlet for the methyl groups. In the $^{13}C\{^1H\}$ NMR spectrum of **4**, the carbenic resonance is observed at 145.2 ppm with ^{195}Pt satellites (J(H,Pt) = 89 Hz).

To obtain Pt^{IV} complexes with a cyclometalated trz ligand, we carried out the reactions of the Pt^{II} complexes *trans-C,C**-**3** and **4** with $PhICl_2$ in 1:1 molar ratio in CH_2Cl_2. On the basis of related precedents,[22,27,28,63] these reactions were expected to proceed with the formal oxidative addition of a Cl^+ ion to form a pentacoordinated cationic Pt^{IV} intermediate and the subsequent electrophilic metalation of the pendant phenyl ring of the trzH ligand, with the release of a proton. In the case of *trans-C,C**-**3**, this reaction did not lead to the cyclometalation of the trzH ligand, but to the complex $[PtCl_3(dtpyH)(trzH)]$ (**5**), in which the trzH ligand is located in cis to both the nitrogen and metalated carbon of the dtpyH ligand (Scheme 1). Reasonably, the cationic Pt^{IV} intermediate resulting from the addition of a Cl^+ ion to complex *trans-C,C**-**3** is very unstable, either because of the mutually trans arrangement of the metalated carbon of the dtpyH ligand and the carbenic carbon or the steric crowding caused by the

nonmetalated tolyl group of the dtpyH ligand, and therefore isomerizes before the metalation of the pendant phenyl ring of the trzH ligand can take place; then, the Cl^- ion liberated by the $PhICl_2$ reagent combines with the metal center to give **5** (Scheme 2). In contrast, the reaction of complex **4** with $PhICl_2$ did allow the cyclometalation of the trzH ligand, but with concomitant demetalation of one of the *p*-tolyl groups of the dtpy ligand to give the bis-cyclometalated complex $[PtCl_2(dtpyH)(trz)]$ (**6**; 68%). In this case, the metalation of the pendant phenyl ring of the trzH ligand may succeed because the cationic intermediate resulting from the addition of Cl^+ to **4** has no possibility to isomerize due to the rigidity imposed by the dicyclometalated dtpy ligand, while the vacant coordination site is blocked by the phenyl ring, preventing the coordination of the liberated Cl^- ion (Scheme 2). After metalation of the phenyl ring, the released proton causes the demetalation of one of the tolyl rings of the dtpy ligand. Similar transcycloplatination processes have been observed upon treatment of complexes of the type $[Pt(C^N^C)(PR_3)]$ (C^N^C = dicyclometalated 2,6-di(*p*-fluorophenyl)pyridine; R = *o*-tolyl, propyl, butyl) with $PhICl_2$, leading to the exchange of a metalated *p*-fluorophenyl ring for a metalated *o*-tolyl, propyl or butyl.[64–66]

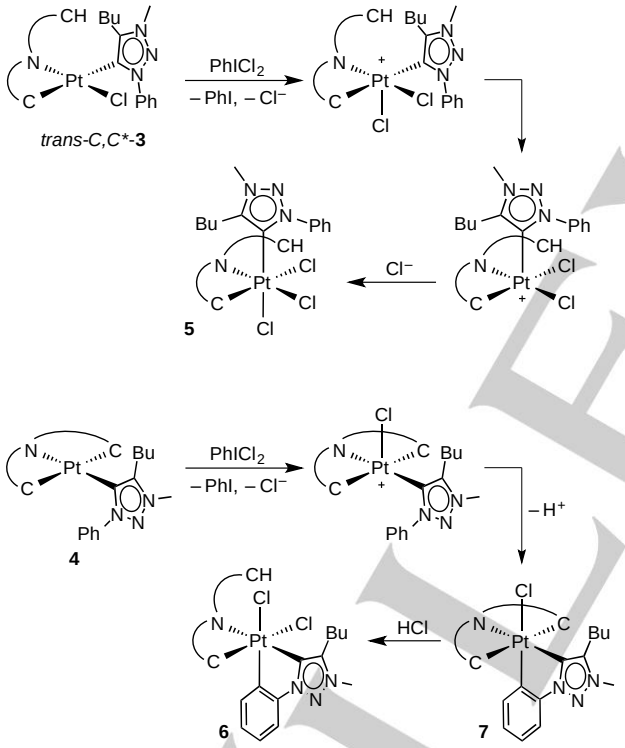

Scheme 2. Proposed reaction pathways for the formation of complexes **5** and **6**.

A clear evidence of the cyclometalation of the trz ligand in **6** is provided by its ^{1}H NMR spectrum, which shows the resonance of the proton in ortho to the metalated phenyl carbon as a doublet of doublets at 5.99 ppm with ^{195}Pt satellites (J(H,Pt) = 42 Hz). The proton in ortho to the metalated carbon of the dtpyH ligand is observed at 6.27 ppm as a singlet with ^{195}Pt satellites (J(H,Pt) = 46 Hz). These protons are significantly shielded relative to the rest of aromatic protons because they are directed toward an aromatic ring (the pyridine or the triazolylidene) and are affected by their ring current (Figure S5).

The ligand arrangement in complex **6** allows the metalation of the second tolyl ring of dtpyH upon treatment with a base. Thus, when **6** is refluxed in acetone at 80 °C in the presence of Na_2CO_3, the tris-cyclometalated complex [PtCl(dtpy)(trz)] (**7**) formed. Complex **7** contains a pincer-C^N^C ligand and a cyclometalated C^C* motif, and the coordination sphere is completed with a chloride ligand. A symmetry plane containing the C^C* ligand makes both metalated tolyl rings equivalent, which is evidenced by the simplicity of the ^{1}H NMR spectrum. The doublet of doublets resonance at 6.25 ppm (J(H,Pt) = 49 Hz) confirms that the phenyl group remains metalated and a singlet with ^{195}Pt satellites at 6.66 ppm (J(H,Pt) = 22 Hz) integrating for two protons evidences the di-metalation of the dtpy ligand.

Crystal Structures

The structures of all the new triazolylidene platinum complexes were unequivocally confirmed by X-ray diffraction studies and are shown in Figure 1. Selected bond lengths and angles are listed in Table 1. The coordination environments deviate appreciably from the ideal square planar (Pt^{II}) or octahedral (Pt^{IV}) geometries, mainly because of the narrow bite angles of the cyclometalating ligands, with N–Pt–C angles in the range 80.0–81.6° and C*–Pt–C angles of about 80.7°. The Pt–C* bond distances are in the range 1.97–2.07 Å and the shortest values are found for complexes with the carbene ligand in trans to the pyridine ring (*i.e., cis-C,C**-**3**, **4**-**6**). A comparison of the structure of complex **5** with that of the bis-cyclometalated complex $[Pt(ppy)_2Cl_2]$ (C_2-symmetrical isomer; ppy = cyclometalated 2-phenylpyridine)[67] evidences the higher trans influence exerted by the triazolylidene ligand relative to the pyridine ring, which results in a Pt–N bond elongation higher than 0.1 Å. The Pt–C bonds lengths involving the metalated aryl rings vary depending on the ligand in trans; the longest values are found for the $Pt–C_{dtpy}$ bond lengths in the C,N,C-pincer complexes **4** (*av.* $Pt–C_{dtpy}$ = 2.057 Å) and **6** (*av.* $Pt–C_{dtpy}$ = 2.091 Å), in which the metalated carbons are mutually trans.

Table 1. Selected bond lengths (Å) and angles (deg) for complexes *trans*/*cis-C,C**-**3**, **4**-**7**.

	*trans-C,C**-**3*	*cis-C,C**-**3*	**4**	**5**	**6**	**7**
Pt–N	2.0457(15)	2.105(2)	2.004(3)	2.0830(13)	2.1507(14)	2.0261(2)
$Pt–C_{dtpy}$	2.0136(18)	1.965(3)	2.052(4) 2.062(3)	2.0086(16)	2.0089(16)	2.094(2) 2.088(2)
Pt–C*	2.0712(18)	1.966(3)	1.974(3)	2.0212(15)	1.9843(16)	1.996(2)
Pt–Cl	2.2983(5)	2.4186(7)	--	2.3122(4) 2.3834(4) 2.4551(4)	2.4223(5) 2.4244(5)	2.4380(5)
$Pt–C_{Ph}$	--	--	--	--	2.0233(17)	2.015(2)
$N–Pt–C_{dtpy}$	80.57(7)	80.58(11)	80.81(14) 80.41(14)	81.61(6)	80.92(6)	80.20(7) 80.00(7)
$C*–Pt–C_{Ph}$	--	--	--	--	80.76(7)	80.73(8)

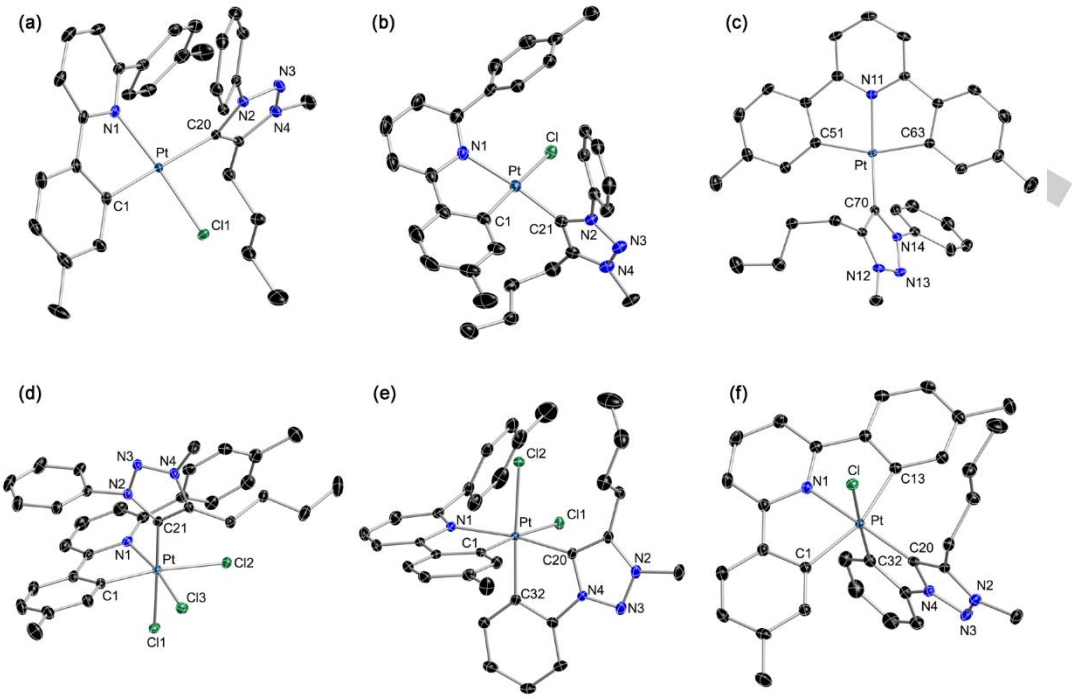

Figure 1. Thermal ellipsoid representations (50% probability) of the crystal structures of *trans-C,C**-**3** (a), *cis-C,C**-**3** (b), **4**·0.5MeCN (c), **5**·2CH_2Cl_2 (d), **6** (e), and **7** (f). Hydrogen atoms and solvent molecules are omitted for clarity.

Photophysical Properties

Although our primary focus is on the photophysical properties of cyclometalated Pt^{IV} complexes, we have included the Pt^{II} precursors *cis/trans-C,C**-**3** and **4** in the photophysical study to compare their properties to those of the Pt^{IV} derivatives. The electronic absorption spectra of *cis/trans-C,C**-**3**, **4**, **5**, **6** and **7** were registered in CH_2Cl_2 solution at 298 K. The resultant data are summarized in Table 2 and the spectra are shown in Figure 2. The lowest-energy feature in the spectra of complexes *cis/trans-C,C**-**3** covers the range 360-450 nm and appears to include several absorptions, whose intensity and energy are typical of primarily ^{1}MLCT transitions usually observed for Pt^{II} complexes with cyclometalated arylpyridines.[68] Similar absorptions have been observed for related complexes of the type *cis-C,C**-[PtCl(C^N)(L)], where C^N is a cyclometalated aryl pyridine and L represents a 2-imidazolylidene ligand.[69]

Table 2. Electronic absorption data for the studied complexes in CH_2Cl_2 solution (*ca.* 5×10^{-5} M) at 298 K.

Complex	λ_{max}/nm ($\varepsilon \times 10^{-2}$/ M^{-1} cm^{-1})
*trans-C,C**-**3**	262 (275), 305 (sh, 140), 351 (sh, 85), 384 (40)
*cis-C,C**-**3**	278 (sh, 111), 330 (101), 402 (24)
4	277 (228), 344 (68), 374 (sh, 47)
5	283 (sh, 119), 324 (74), 352 (69), 368 (sh, 58)
6	259 (201), 317 (84), 344 (98)
7	323 (152), 347 (72), 365 (68), 384 (55)

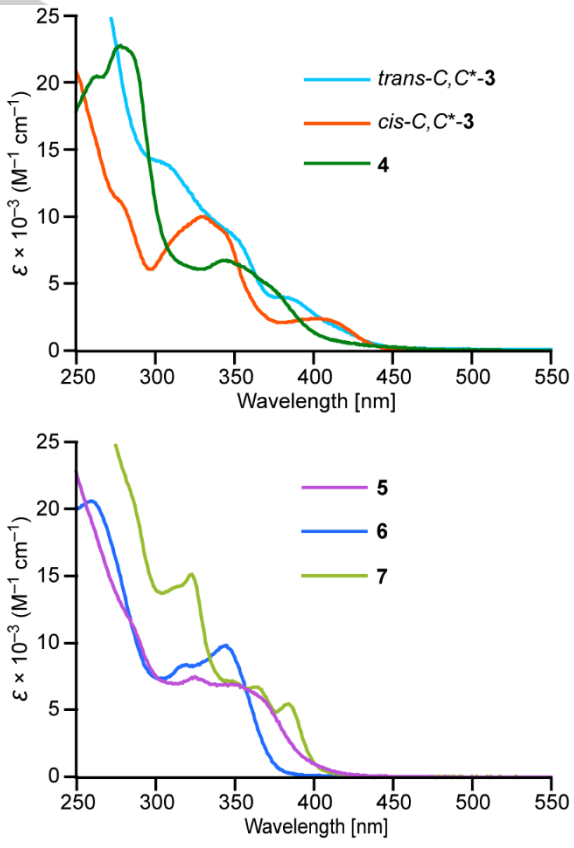

Figure 2. Electronic absorption spectra of *cis/trans-C,C**-**3** and **4**–**7** in CH_2Cl_2 solution at 298 K.

The main features observed in the spectrum of **4** are typical of complexes of the type [Pt(C^N^C)L].[70–72] The moderately intense absorptions in the range 330-400 nm can be ascribed mainly to ^{1}LC transitions within the dtpy ligand, and the long tail in the range 400-500 nm to primarily ^{1}MLCT transitions involving the same ligand. A very weak absorption can be also observed at 513 nm, which can be assigned to a spin-forbidden ^{3}MLCT absorption on the basis of related precedents (Figure S7).

Complex **5** gives absorptions in the range 300-380 nm that can be ascribed to ^{1}LC transitions within the dtpyH ligand, while the long tail extending to ca. 450 nm is typical of LMCT and/or LLCT transitions, as has been observed for other Pt^{IV} complexes with halide ligands.[23] Complexes **6** and **7** give rise to several absorptions in the ranges 300-380 nm and 300-400 nm, respectively, that can be assigned to ^{1}LC transitions within the cyclometalated ligands. ^{1}MLCT transitions are not expected for these complexes in the near UV or visible regions because the occupied d orbitals in Pt^{IV} lie at very low energies.

The luminescence of complexes *cis-C,C**-**3**, **6** and **7** was examined in deaerated CH_2Cl_2 solutions and poly(methyl methacrylate) (PMMA) thin films at 298 K and in frozen butyronitrile (PrCN) glasses at 77 K. Complex *trans-C,C**-**3** was not investigated because of its photolabile nature. Complex **4** does not emit in CH_2Cl_2 at 298 K when excited at the lowest-energy absorption band, while it produces a weak orange-red luminescence in the solid state and frozen PrCN, that must arise from molecular aggregates, as has been found for other complexes of the type [Pt(C^N^C)L][70–72] (see the SI for details). Complex **5** does not emit in CH_2Cl_2 at 298 K, presumably because of the presence of low-lying LMCT excited states, and was not further investigated. Complexes *cis-C,C**-**3**, **6** and **7** are luminescent in all the employed media and their emission data are summarized in Table 3. Figure 3 shows the emission spectra in PMMA at 298 K, which are almost identical to those in CH_2Cl_2 solution. The complete set of excitation and emission spectra are given in the SI. The Pt^{IV} complexes **6** and **7** exhibit highly structured emissions in the blue-green region, with lifetimes in the tens to hundreds of microseconds range, which are consistent with triplet emitting excited states of predominantly ligand-centered character (^{3}LC), as has been found for previously reported bis- and tris-cyclometalated Pt^{IV} complexes with arylpyridines.[23,25,28,29] The observed emission energies are similar to those of ^{3}LC emitters of the types [Au(C^N^CH)(O_2CCF_3)(R)] or [Au(C^N^C)(R)], where C^N^C or C^N^CH represents mono- or dicyclometalated 2,6-bis(4-(*tert*-butyl)phenyl)pyridine, respectively,[73,74] suggesting that the involved ligand is dtpyH in **6** and dtpy in **7**; these ligands are expected to have lower π-π^* transition energies than the cyclometalated trz ligand because of their more extended π conjugation. Complex *cis-C,C**-**3** displays a broader emission band, with a lower energy and shorter lifetime compared to the Pt^{IV} complexes, indicating an emitting state of mixed ^{3}LC/MLCT character, which is typical of Pt^{II} complexes with chelating heteroaromatic ligands.[68]

Complex **6** is the most efficient emitter of the studied series. Its quantum yield in fluid CH_2Cl_2 solution at 298 K (Φ = 0.15) is higher than that of [Pt(ppy)$_2$Cl$_2$] (C_2-symmetrical isomer, Φ = 0.11),[23] which means that the replacement of a cyclometalated arylpyridine by a cyclometalated arylcarbene has a beneficial effect on the luminescence of this type of bis-cyclometalated Pt^{IV} complexes. A comparison of the radiative and nonradiative rate constants (k_r and k_{nr}) with those of [Pt(ppy)$_2$Cl$_2$] reveals that this enhancement in quantum efficiency is attributable to an appreciable decrease in k_{nr} (13×10^{-3} vs 33×10^{-3} s^{-1}), while there is a relatively small decrease in k_r (2.3×10^{-3} vs 4.2×10^{-3} s^{-1}).

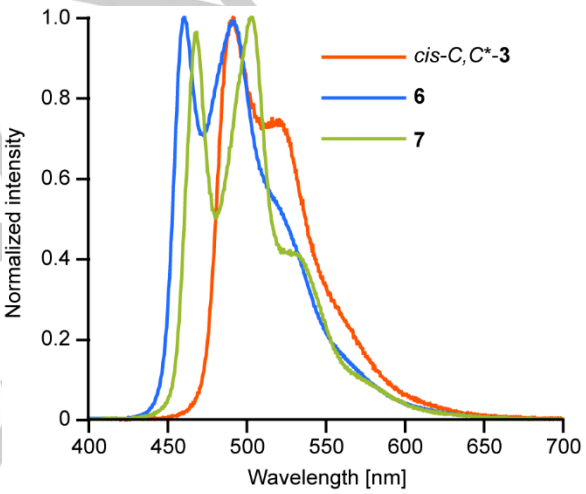

Figure 3. Emission spectra of *cis-C,C**-**3**, **6** and **7** in PMMA (2 wt%) at 298 K.

In comparison with **6**, complex **7** displays a considerably lower quantum yield in CH_2Cl_2, which means that dicyclometalation of the diarylpyridine ligand has a detrimental effect on the luminescence. A similar observation has been previously noted for Au(III) complexes with mono- or dicyclometalated 2,6-diarylpyridine ligands, the former showing significantly higher emission efficiencies in solution.[74] The low quantum efficiency of **7** in fluid solution is mainly attributable to its k_r, which is one order of magnitude smaller than those found for **6** and related bis-cyclometalated Pt^{IV} complexes.[23] Comparably low k_r values have been found for meridional isomers of heteroleptic tris-cyclometalated Pt^{IV} complexes, *mer*-[Pt(C^N)$_2$(C'^N')]$^+$,[29] suggesting that the mutually trans arrangement of a pair of metalated carbons could be associated with a less effective SOC induced by the metal.

Complex *cis-C,C**-**3** presents the highest k_{nr} value of the studied series in CH_2Cl_2 at 298 K and a lower than expected k_r value, resulting in a very

Table 3. Emission data of *cis-C,C**-**3**, **6** and **7**.

Complex	Medium (T [K])	λ_{em} [nm][a]	Φ[b]	τ [µs][c]	$k_r \times 10^{-3}$ [s^{-1}][d]	$k_{nr} \times 10^{-3}$ [s^{-1}][e]
*cis-C,C**-**3**	CH_2Cl_2 (298)	*492*, 519	0.0032	7.6	0.42	131
	PMMA (298)	*492*, 519	0.35	13	27	50
	PrCN (77)	*481*, 517, 553 (sh)	-	19	-	-
6	CH_2Cl_2 (298)	*462*, 494, 524 (sh)	0.15	65	2.3	13
	PMMA (298)	*461*, 492, 520 (sh)	0.71	288	2.5	1.0
	PrCN (77)	*455*, 488, 514	-	462	-	-
7	CH_2Cl_2 (298)	469, *504*, 531	0.0032	16	0.20	62
	PMMA (298)	468, *503*, 531	0.61	252	2.4	1.5
	PrCN (77)	464, *499*, 527	-	387	-	-

[a] The most intense peak is italicized. [b] Quantum yield. [c] Emission lifetime. [d] Radiative rate constant, $k_r = \Phi/\tau$. [e] Nonradiative rate constant, $k_{nr} = (1 - \Phi)/\tau$.

weak emission. Related complexes of the type *cis*-*C,C**-[PtCl(C^N)(L)] exhibit quantum yields in the range Φ = 0.054-0.079 in the same medium.[69]

The three complexes display considerably enhanced emissions in PMMA films (2 wt%) at 298 K; the Pt^{IV} complexes **6** and **7** are significantly more efficient than the Pt^{II} complex *cis*-*C,C**-**3** in this medium, and **6** (Φ = 0.71) even surpasses tris-cyclometalated complexes of the type *fac*-$[Pt(C^N)_3]^+$ (range Φ = 0.16-0.61).[28] Large increases in quantum efficiencies upon immobilization in PMMA have been previously observed for cyclometalated Ir^{III}[75] and Pt^{II}[76] complexes, associated with a decrease in k_{nr} that, in some cases, may combine with an enhancement of k_r. In the case of complex **6**, its k_r value in PMMA is very similar to that in CH_2Cl_2, but its k_{nr} decreases by an order of magnitude upon immobilization, indicating that in this case the suppression of nonradiative deactivation due to molecular motion is the dominant factor explaining the dramatic increase in quantum efficiency in PMMA. In the case of **7**, both a substantial increase in k_r and a decrease in k_{nr} occur upon immobilization; the former may imply that the PMMA matrix favors geometry variations in the exited state that enhance the SOC effects induced by the metal or that these effects are compromised by certain molecular vibrations that are inhibited in the rigid medium.

Computational Study

To get an understanding of the nature of their emissive excited states, DFT and TDDFT calculations have been performed for complexes **6** and **7** at the B3LYP/(6-31G**+LANL2DZ) level considering solvent effects (CH_2Cl_2). Isodensity surfaces of frontier molecular orbitals and a diagram comparing their energies are shown in Figures 4 and 5, respectively. The compositions of the molecular orbitals from atomic orbital contributions are given in the Supporting Information (SI). The most relevant singlet and triplet excitations obtained from TDDFT calculations at the optimized ground state geometries in CH_2Cl_2 are given in Table 4 and a more extensive listing is included in the SI.

The highest occupied molecular orbital (HOMO) and the HOMO–1 in complex **6** are mainly comprised of π orbitals of the dtpyH ligand with an appreciable contribution from the Cl ligand (11% and 27%, respectively), and some metal orbital character (2% and 4%), while the lowest unoccupied molecular orbital (LUMO) and the LUMO+1 are composed of π* orbitals of both the dtpyH and trz ligands and have a 5% metal orbital contribution. The lowest-energy singlet excitations in this complex involve electronic transitions from the HOMO or HOMO–1 to the LUMO or LUMO+1, and therefore have a mixed ligand centered/ligand-to-ligand charge-transfer character (^{1}LC/LLCT). The main monoexcitations contributing to the lowest triplet are HOMO-LUMO and HOMO-LUMO+1 transitions, and thus it can be similarly designated as ^{3}LC/LLCT.

In complex **7**, the HOMO and HOMO–1 are π orbitals of the dtpy ligand. They lie at higher energies and have higher metal orbital contributions (4 and 10%, respectively) relative to those in **6**. The LUMO is a π* orbital on the trz ligand, while the LUMO+*n* (*n* = 1, 2) are π* orbitals on the dtpy ligand. The two lowest-energy singlet excitations correspond to LC transitions within the dtpy ligand (HOMO-LUMO+1 and HOMO–1-LUMO+1). The lowest triplet excitation arises also from a LC(dtpy) transition (HOMO-LUMO+2).

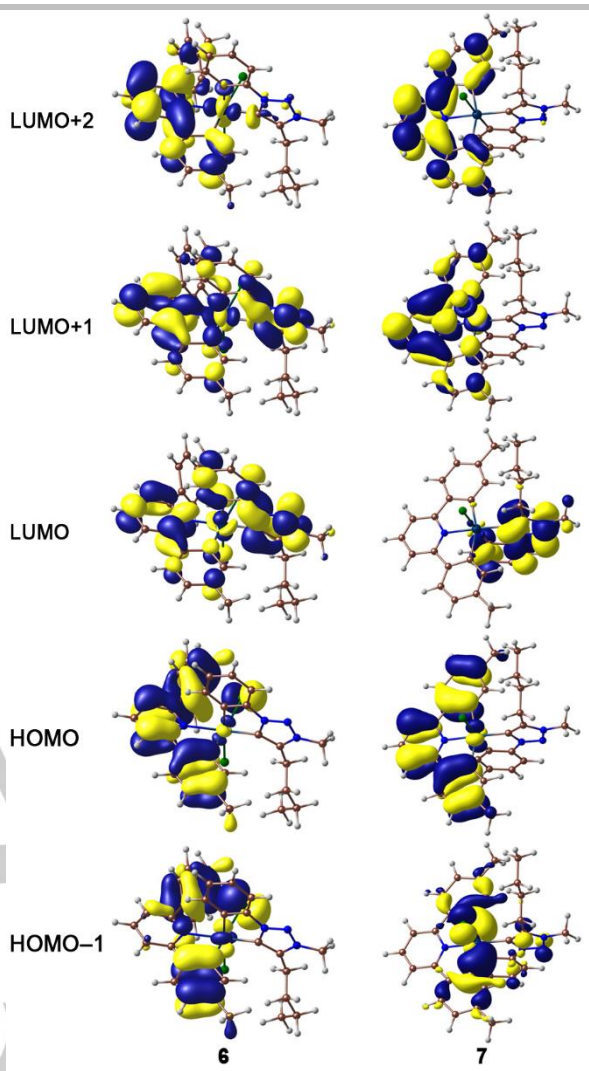

Figure 4. Selected molecular orbital isosurfaces (0.03 e bohr^{-3}) for **6** and **7**.

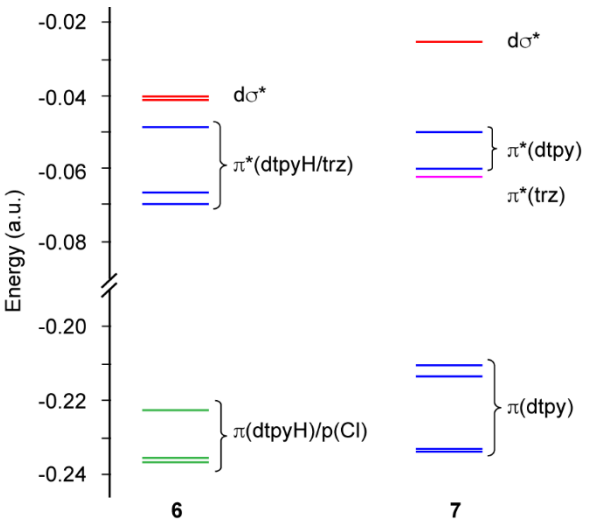

Figure 5. Orbital energy diagrams from DFT calculations for complexes **6** and **7** in CH_2Cl_2 solution.

Table 4. Selected vertical singlet and triplet excitations of **6** and **7** from TD-DFT calculations at the S_0 geometry in CH_2Cl_2.

Compd	State	Main monoexcitations[a]	ΔE/eV	λ/nm	Oscillator strength	Main character
6	S_1	H → L (64%) H → L+1 (31%)	3.532	351.1	0.1779	LC(dtpyH)/LLCT(dtpyH→trz)
	S_2	H → L (30%) H → L+1 (63%)	3.669	338.0	0.0175	LC(dtpyH)/LLCT(dtpyH→trz)
	S_3	H–1 → L (76%)	3.877	319.8	0.0133	LC(dtpyH)/LLCT(dtpyH,Cl→trz)
	S_4	H–3 → L (17%) H–2 → L (37%) H–1 → L (12%) H–1 → L+1 (15%)	3.941	314.6	0.0324	LC(dtpyH)/LLCT(dtpyH,Cl→trz)
	T_1	H → L (26%) H → L+1 (23%) H → L+2 (13%)	2.853	434.5	-	LC(dtpyH)/LLCT(dtpyH→trz)
	T_{14}	H–2 → L (5%) H–2 → L+1 (5%) H–1 → L (8%) H → L+3 (19%)	3.963	312.9	-	LC(dtpyH)/LLCT(dtpyH,Cl→trz)/LMCT
7	S_1	H–1 → L+1 (72%) H → L+1 (25%)	3.326	372.8	0.0122	LC(dtpy)
	S_2	H–1 → L+1 (26%) H → L+1 (71%)	3.382	366.6	0.0843	LC(dtpy)
	S_3	H–1 → L (94%) H → L (4%)	3.510	353.2	0.0395	LLCT(dtpy→trz)
	S_6	H → L+2 (84%)	4.018	308.6	0.1538	LC(dtpy)
	T_1	H–2 → L+1 (11%) H → L+2 (71%)	2.779	446.2	-	LC(dtpy)
	T_{13}	H–4 → L+1 (21%) H–1 → L+3 (45%) H → L+3 (9%)	3.877	319.8	-	LMCT

[a] H = HOMO; L = LUMO.

Thermal population of ^{3}LMCT excited states from the lowest triplet state has been previously identified a major nonradiative deactivation channel in some cyclometalated Pt^{IV} complexes.[23,29] The formation of these states involves electronic promotions to dσ* orbitals. In complexes **6** and **7**, the dσ* orbitals lie at relatively high energies (LUMO+3 and LUMO+4 in complex **6**; LUMO+3 in complex **7**) and the lowest vertical triplet excitations with a significant LMCT character can be found at 3.96 eV for **6** (T_{14}) or 3.88 eV for **7** (T_{13}), that is, 1.1 eV above the lowest triplet state in both cases. This energy difference is significantly higher than that found for $[PtCl_2(ppy)_2]$ (0.60 eV),[23] suggesting that nonradiative deactivation through the thermal population of these states could be relatively unimportant, as is the case of the heteroleptic tris-cyclometalated complexes *mer*-$[Pt(ppy)_2(thpy)]^+$ (1.15 eV; thpy = cyclometalated 2-(2-thienyl)pyridine) and *mer*-$[Pt(ppy)_2(piq)]^+$ (1.27 eV; piq = cyclometalated 1-phenylisoquinoline),[29] which is consistent with the relatively low values found for k_{nr}.

The geometry of the lowest triplet excited state (T_1) in CH_2Cl_2 solution was optimized for both complexes. The calculated electronic energies with respect to the ground state (adiabatic energy differences) are 2.72 (**6**) and 2.70 eV (**7**), in good agreement with the observed emission energies. Figure 6 shows the spin density distribution of the optimized triplet state of each complex. Although the vertical excitation leading to T_1 in complex **6** has a mixed LC/LLCT character, the spin density distribution of the relaxed state matches the topology of a π-π* transition within the dtpyH ligand, and therefore the emitting state should be designated as ^{3}LC(dtpyH), while the cyclometalated trz acts as a nonchromophoric ligand. Consistently, the geometry modifications with respect to the ground state affect only the metallacyclic portion of the dtpyH ligand (see the SI for further details). A comparable scenario is found in the lowest triplet of complex **7**, where the spin density is not evenly distributed over the dtpy ligand, but mainly over the pyridine moiety and one of the metalated tolyl rings, resulting in significant geometry modifications only on this portion of the tridentate ligand (see the SI); notwithstanding, the resulting distortions do not lead to the loss of planarity of this ligand, which contrasts with the highly distorted, nonplanar geometries found for the lowest triplet in Pt^{II} complexes with C^N^C ligands.[31] The spin densities on the Pt atom (0.017 for **6** and 0.029 for **7**) are comparable to those found for different types of neutral, bis-cyclometalated Pt^{IV} complexes (range 0.027-0.050),[23] and indicate a small degree of metal orbital involvement and hence a certain admixture of MLCT character into the emitting state.

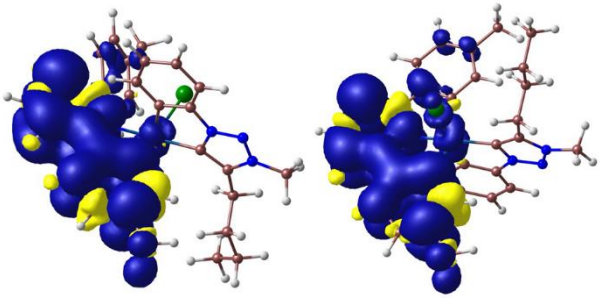

Figure 6. Spin density distributions (0.0008 e bohr^{-3}) of the optimized lowest triplet excited state of **6** (left) and **7** (right).

Conclusions

A synthetic route to Pt^{IV} complexes bearing a cyclometalated triazolylidene and a bi- or terdentate 2,6-diarylpyridine ligand has been established. The targeted complexes are the first examples of Pt^{IV} species bearing a cyclometalated mesoionic aryl-NHC ligand. In addition to them, the Pt^{II} precursors containing bi- or terdentate 2,6-diarylpyridine and the coordinated triazolylidene have been completely characterized.

The Pt^{IV} complexes **6** and **7** show moderate or weak emissions, respectively, in fluid solution at 298 K, arising from ^{3}LC states involving the dtpyH or dtpy ligand. The luminescence of the bis-cyclometalated complex **6** in solution is enhanced with respect to $[Pt(ppy)_2Cl_2]$, indicating that the cyclometalated trz ligand has a beneficial effect. Although the C^N^C coordination of the dtpy ligand in **7** apparently has a detrimental effect on its emission efficiency in fluid solution, both **6** and **7** display exceptionally intense emissions in rigid PMMA matrices, which are comparable or higher than those found for tris-cyclometalated complexes of the type *fac*-$[Pt(C^N)_3]^+$. The computational study confirms that the cyclometalated trz ligand induces a higher ligand-field splitting relative to 2-arylpiridines, thereby increasing the energies of dσ* orbitals and deactivating LMCT states. The examined Pt^{II} complexes bearing a coordinated trz ligand, *cis-C,C**-**3** and **4**, are less suited systems to produce efficient luminescence.

In brief, the present work establishes a route to cyclometalated Pt^{IV} complexes with 3 or 4 carbon donor moieties, demonstrates for the first time the benefits of using cyclometalated aryl-NHC supporting ligands in Pt^{IV} to obtain efficient luminescence, and opens the way to the development of new types of aryl-NHC Pt^{IV} emitters.

Experimental Section

General considerations and materials

Unless otherwise noted, preparations were carried out at room temperature under atmospheric conditions. Synthesis grade solvents were obtained from commercial sources and used without further purification. Reactions involving silver reagents were carried out under a N_2 atmosphere in the dark. $PhICl_2$[77] and the triazolium iodide salt[78] were prepared following reported procedures. The preparations of $[Pt_2(\mu\text{-}Cl)_2(dtpyH)_2]$ (**1**) and [Pt(dtpy)(DMSO)] (**2**) follow the procedures reported for the analogous 2,6-diphenylpyridine complexes and are given in the SI. All other reagents were obtained from commercial sources. The experimental setup employed for the photoisomerizarion reaction has been previously described.[61] NMR spectra were recorded on Bruker Advance 300 or 400 MHz spectrometers at 298 K. Chemical shifts (δ) were referenced to residual signals of non-deuterated solvent and are given in ppm downfield from tetramethylsilane. Elemental analyses were carried out with a LECO CHNS-932 microanalyzer.

Synthesis of *trans-C,C**-[PtCl(dtpyH)(trzH)] (*trans-C,C**-3)

The triazolium salt (200 mg, 0.58 mmol) and Ag_2O (270 mg, 1.16 mmol) were suspended in CH_2Cl_2 (10 mL) and the mixture was stirred at room temperature for 14 h in the absence of light and under a N_2 atmosphere. The suspension was filtered through Celite and $[Pt_2(\mu\text{-}Cl)_2(dtpyH)_2]$ (**1**) (284 mg, 0.29 mmol) was immediately added to the filtrate. The mixture was stirred for 1 h at room temperature, filtered through Celite and concentrated to *ca.* 3 mL under reduced pressure. The addition of pentane led to the precipitation of a yellow solid, which was filtered off and vacuum-dried to give *trans-C,C**-**3**. Yield: 374 mg, 91%. ^{1}H NMR (300 MHz, CD_2Cl_2): *δ*=8.42–8.37 (m, 2H; H_{arom}), 7.84 (br s with satellites, *J*(H,Pt)=23 Hz, 1H; H_{arom}), 7.59 (br d, *J*(H,H)=8.0 Hz, 1H; H_{arom}), 7.50 (t, *J*(H,H)=7.8 Hz, 1H; H_{arom}), 7.40 (d, *J*(H,H)=8.2 Hz, 2H; H_{arom}), 7.26–7.19 (m, 3H; H_{arom}), 7.13 (br d, *J*(H,H)=7.6 Hz, 1H; H_{arom}), 7.02 (br d, *J*(H,H)=7.5 Hz, 1H; H_{arom}), 6.96–6.92 (m, 1H; H_{arom}), 6.87 (br d, *J*(H,H)=7.6 Hz, 1H; H_{arom}), 6.63 (dd with satellites, *J*(H,H)=7.5, 1.5 Hz, *J*(H,Pt)=25 Hz, 1H; H_{arom}), 3.77 (s, 3H; NCH_3), 3.11–3.01 (m, 1H; CH_2), 2.37 (s, 3H; CH_3), 2.36 (s, 3H; CH_3), 2.05–1.90 (m, 2H; CH_2), 1.60–1.37 (m, 3H; CH_2), 1.00 (t, *J*(H,H)=7.2 Hz, 3H; CH_3); ^{13}C NMR (75 MHz, CD_2Cl_2): *δ*=169.9 (C), 169.6 (C), 162.3 (C), 161.3 (C), 148.3 (*J*(C,Pt)=40 Hz; C), 145.0 (*J*(C,Pt)=38 Hz; C), 139.7 (C), 139.3 (C), 138.7 (C), 138.2 (C), 137.0 (CH), 135.5 (*J*(C,Pt)=47 Hz; CH), 130.0 (CH), 129.2 (CH), 128.8 (CH), 128.5 (CH), 128.2 (CH), 125.3 (CH), 124.5 (CH), 124.0 (CH), 123.9 (CH), 122.0 (CH), 116.3 (*J*(C,Pt)=40 Hz; CH), 36.1 (NCH_3), 32.0 (CH_2), 26.9 (CH_2), 23.6 (CH_2), 22.2 (CH_3), 21.6 (CH_3), 14.2 (CH_3); elemental analysis calcd (%) for $C_{32}H_{33}ClN_4Pt$: C 54.58, H 4.72, N 7.96; found: C 54.59, H 4.64, N 7.72.

Synthesis of *cis-C,C**-[PtCl(dtpyH)(trzH)] (*cis-C,C**-3)

A deareated solution of *trans-C,C**-**3** (35 mg, 0.05 mmol) in acetone (10 mL) was irradiated with blue LEDs for 20 h under a N_2 atmosphere with vigorous stirring. NH_4Cl (16 mg, 0.30 mmol) was then added and the mixture was stirred for 15 min. The solvent was evaporated to dryness and the residue was extracted with CH_2Cl_2 (2 × 3 mL). The solution was concentrated under reduced pressure (2 mL) and Et_2O (15 mL) was added, whereupon a pale yellow solid precipitated, which was filtered off and vacuum-dried to give *cis-C,C**-**3**. Yield: 21 mg, 60%. ^{1}H NMR (300 MHz, CD_2Cl_2): δ=8.37–8.33 (m, 2H; H_{arom}), 7.86–7.78 (m, 3H; H_{arom}), 7.65 (dd, *J*(H,H)=8.0, 1.4 Hz, 1H; H_{arom}), 7.52–7.45 (m, 1H; H_{arom}), 7.37–7.33 (m, 2H; H_{arom}), 7.23–7.19 (m, 2H; H_{arom}), 6.77 (br d, *J*(H,H)=7.9 Hz, 1H; H_{arom}), 6.22 (br s with satellites, *J*(H,Pt)=69 Hz, 1H; H_{arom}), 4.12 (s, 3H; NCH_3), 3.14–3.03 (m, 1H; CH_2), 2.80–2.69 (m, 1H; CH_2), 2.42 (s, 3H; CH_3), 2.09 (s, 3H; CH_3), 1.85–1.72 (m, 1H; CH_2), 1.72–1.59 (m, 1H; CH_2), 1.38–1.27 (m, 2H; CH_2), 0.83 (t, *J*(H,H)=7.3 Hz, 3H; CH_3); ^{13}C NMR (75 MHz, CD_2Cl_2): δ=166.5 (C), 162.4 (C), 145.8 (C), 143.6 (C), 140.6 (C), 139.3 (C), 138.8 (C), 138.4 (CH), 135.9 (CH), 129.9 (CH), 129.7 (CH), 129.0 (CH), 128.6 (CH), 125.5 (CH), 124.4 (CH), 123.5 (CH), 123.4 (CH), 115.9 (CH), 37.1 (NCH_3), 30.7 (CH_2), 25.7 (CH_2), 23.2 (CH_2), 21.8 (CH_3), 14.1 (CH_3); elemental analysis calcd (%) for $C_{32}H_{33}ClN_4Pt$: C 54.58, H 4.72, N 7.96; found: C 54.48, H 4.78, N, 7.82.

Synthesis of [Pt(dtpy)(trzH)] (4)

Method A. Complex *trans-C,C**-**3** (150 mg, 0.21 mmol) and $NaOAc{\cdot}3H_2O$ (145 mg, 1.07 mmol) were suspended in acetone (40 mL) under a N_2 atmosphere and the mixture was irradiated with blue LEDs for 20 h with vigorous stirring. The suspension was filtered through Celite and the filtrate was concentrated (3 mL). The addition of pentane (20 mL) led to the precipitation of an orange solid, which was filtered off and vacuum-dried to give 4. Yield: 98 mg, 69%. *Method B.* The triazolium salt (80 mg, 0.23 mmol) and Ag_2O (108 mg, 0.47 mmol) were suspended in CH_2Cl_2 (10 mL) and the reaction mixture was stirred at room temperature under a N_2 atmosphere for 14 h in the absence of light. The mixture was filtered through Celite and complex **2** (124 mg, 0.23 mmol) was immediately added. The resulting mixture was deoxygenated and stirred in the dark at room temperature for 14 h. The mixture was filtered through Celite and concentrated (3 mL). The addition of pentane led to the precipitation of an orange solid, which was filtered off and vacuum-dried to give **4** (135 mg, 87%). ^{1}H NMR (300 MHz, CD_2Cl_2): δ=8.49–8.45 (m, 2H; H_{arom}), 7.52 (dd, *J*(H,H)=8.3, 7.6 Hz, 1H; H_{arom}), 7.40–7.29 (m, 5H, H_{arom}), 7.23–7.18 (m, 2H; H_{arom}), 6.84–6.72 (m, 4H, H_{arom}), 4.23 (s, 3H; NCH_3), 2.91 (t, *J*(H,H)=7.5 Hz, 2H; CH_2), 2.13 (s, 6H, CH_3), 1.74 (quint, 2H; CH_2), 1.35–1.22 (m, 2H; CH_2), 0.78 (t, *J*(H,H)=7.4 Hz, 3H; CH_3); ^{13}C NMR (75 MHz, CD_2Cl_2): δ=176.1 (C), 171.4 (C), 167.1 (*J*(C,Pt)=65 Hz; C), 157.5 (C), 148.1 (*J*(C,Pt)=30 Hz; C), 145.2 (*J*(C,Pt)=89 Hz, C_{trz}–Pt), 140.0 (*J*(C,Pt)=39 Hz; C), 139.2 (CH), 139.1 (CH), 129.1 (CH), 128.9 (CH), 124.2 (CH), 124.1 (CH), 123.7 (CH), 114.0 (*J*(C,Pt)=25 Hz; CH), 37.0 (NCH_3), 30.7 (CH_2), 26.3 (CH_2), 22.9 (CH_2), 22.0 (CH_3), 21.7 (CH_3), 14.1 (CH_3);

elemental analysis calcd (%) for $C_{32}H_{32}N_4Pt$: C 57.56, H 4.83, N 8.39; found: C 57.47, H 4.73, N, 8.13.

Synthesis of [$PtCl_3$(dtpyH)(trzH)] (5)

To a solution of *trans-C,C**-**3** (60 mg, 0.085 mmol) in CH_2Cl_2 (5 mL) was added $PhICl_2$ (23 mg, 0.085 mmol) and the mixture was stirred at room temperature for 30 min. The mixture was concentrated under reduced pressure (2 mL) and Et_2O (20 mL) was added, whereupon a pale-yellow precipitate formed, which was filtered off and vacuum-dried to give **5**. Yield: 40 mg, 61%. ^{1}H NMR (400 MHz, CD_2Cl_2): δ=7.79 (t, *J*(H,H)=7.8 Hz, 1H; H_{arom}), 7.51 (s with satellites, *J*(H,Pt)=25 Hz, 1H; H_{arom}), 7.45 (dd, *J*(H,H)=8.1, 1.4 Hz, 1H; H_{arom}), 7.19–7.14 (m, 3H; H_{arom}), 7.08 (br, 2H; H_{arom}), 6.95–6.81 (m, 4H; H_{arom}), 6.64 (br, 1H; H_{arom}), 6.53 (br, 1H; H_{arom}), 6.36 (br, 1H; H_{arom}), 4.22 (s, 3H; NCH_3), 3.97–3.86 (m, 1H; CH_2), 3.03 (ddd, *J*(H,H)=15.5, 13.1, 3.4 Hz, 1H; CH_2), 2.42 (s, 3H; CH_3), 2.38 (s, 3H; CH_3), 1.83–1.72 (m, 1H; CH_2), 1.57–1.40 (m, 3H; CH_2), 0.99 (t, *J*(H,H)=7.0 Hz, 3H; CH_3). ^{13}C NMR (100 MHz, CD_2Cl_2): δ=167.5 (C), 163.1 (C), 150.1 (C), 143.4 (C), 141.6 (C), 140.1 (CH), 139.4(C), 138.1 (C), 137.6 (C), 131.5 (*J*(C,Pt)=26 Hz; CH), 129.8 (CH), 129.4 (CH), 129.2 (CH), 128.9 (CH), 128.5 (*J*(C,Pt)=25 Hz; CH), 128.2 (CH), 128.0 (CH), 127.1 (CH), 126.6 (*J*(C,Pt)=23 Hz; CH), 124.2 (CH), 119.8 (*J*(C,Pt)=25 Hz; CH), 38.0 (NCH_3), 31.9 (CH_2), 26.7 (CH_2), 23.2 (CH_2), 22.2 (CH_3), 21.6 (CH_3), 14.5 (CH_3); elemental analysis calcd (%) for $C_{32}H_{33}ClN_4Pt$: C 49.59, H 4.29, N 7.23; found: C 49.52, H 4.20, N, 7.38.

Synthesis of [$PtCl_2$(dtpyH)(trz)] (6)

To a solution of **4** (75 mg, 0.11 mmol) in CH_2Cl_2 (5 mL) was added $PhICl_2$ (50 mg, 0.18 mmol) and the mixture was stirred for 10 min. Partial evaporation of the resulting solution under reduced pressure (2 mL) and addition of Et_2O (20 mL) led to the precipitation of a pale-yellow solid, which was filtered off and vacuum-dried to give **6**·0.25CH_2Cl_2. Yield: 57 mg, 68%. ^{1}H NMR (400 MHz, CD_2Cl_2): δ=8.05–7.97 (m, 2H; H_{arom}), 7.72 (br, 2H; H_{arom}), 7.58 (d with satellites, *J*(H,H)=8.0 Hz, *J*(H,Pt)=4 Hz, 1H; H_{arom}), 7.51–7.46 (m, 1H; H_{arom}), 7.37 (dd with satellites, *J*(H,H)=7.0, 2.2 Hz, *J*(H,Pt)=7 Hz, 1H; H_{arom}), 7.18 (d, *J*(H,H)=8.1 Hz, 2H; H_{arom}), 7.07 (td, *J*(H,H)=7.7, 1.2 Hz, 1H; H_{arom}), 6.94 (d, *J*(H,H)=8.0 Hz, 1H; H_{arom}), 6.93–6.87 (m, 1H; H_{arom}), 6.27 (s with satellites, *J*(H,Pt)=46 Hz, 1H; H_{arom}), 5.99 (dd with satellites, *J*(H,H)=7.9, 1.2 Hz, *J*(H,Pt)=42 Hz, 1H; H_{arom}), 4.23 (s, 3H; NCH_3), 3.71 (m, 1H; CH_2), 3.07 (m, 1H; CH_2), 2.37 (s, 3H; CH_3), 2.14 (s, 3H; CH_3), 1.89–1.76 (m, 2H; CH_2), 1.58–1.48 (m, 2H; CH_2), 1.01 (t, *J*(H,H)=7.4 Hz, 3H; CH_3). ^{13}C NMR (100 MHz, CD_2Cl_2): δ=165.1 (C), 164.4 (C), 143.4 (*J*(C,Pt)=83 Hz, C_{trz}–Pt), 142.2 (C), 141.0 (C), 139.6 (CH), 139.5(C), 139.4 (C), 139.1 (C), 137.8 (C), 132.0 (*J*(C,Pt)=57 Hz; CH), 130.1 (*J*(C,Pt)=42 Hz; CH), 130.0 (C), 129.8 (CH), 128.5 (CH), 128.0 (*J*(C,Pt)=10 Hz; CH), 126.8 (CH), 126.1 (CH), 126.0 (CH), 119.5 (*J*(C,Pt)=20 Hz; CH), 115.8 (*J*(C,Pt)=32 Hz; CH), 37.6 (NCH_3), 31.4 (CH_2), 24.1 (CH_2), 23.2 (CH_2), 21.9 (CH_3), 21.7 (CH_3), 14.1 (CH_3); elemental analysis calcd (%) for $C_{32}H_{32}Cl_2N_4Pt$·0.25CH_2Cl_2: C 50.98, H 4.31, N 7.37; found: C 50.91, H 4.31, N, 7.23.

Synthesis of [PtCl(dtpy)(trz)] (7)

Complex **6** (52 mg, 0.07 mmol) and Na_2CO_3 (37 mg, 0.35 mmol) were suspended in acetone (10 mL) under a N_2 atmosphere and the mixture was stirred in a sealed tube at 80 °C for 14 h. The suspension was filtered through Celite and the filtrate was concentrated under reduced pressure (3 mL). The addition of pentane (15 mL) led to the precipitation of a pale yellow solid, which was filtered off and vacuum-dried to give **7**. Yield: 40 mg, 81%. ^{1}H NMR (300 MHz, CD_2Cl_2): δ=7.94 (t, *J*(H,H)=8.1 Hz, 1H; H_{arom}), 7.65 (d, *J*(H,H)=8.0 Hz, 2H; H_{arom}), 7.60 (d, *J*(H,H)=8.0 Hz, 3H; H_{arom}), 7.02 (td, *J*(H,H)=7.8, 1.2 Hz, 2H; H_{arom}), 6.88 (dd, *J*(H,H)=7.9, 1.2 Hz, 2H; H_{arom}), 6.82–6.74 (m, 1H; H_{arom}), 6.65 (s with satellites, *J*(H,Pt)=22 Hz, 2H; H_{arom}), 6.25 (dd with satellites, *J*(H,H)=7.8, 1.2 Hz, *J*(H,Pt)=49 Hz, 1H; H_{arom}), 4.35 (s, 3H; NCH_3), 3.44 (t, *J*(H,H)=7.8 Hz, 2H; CH_2), 2.14 (s, 6H, CH_3), 1.92–1.82 (m, 2H; CH_2), 1.57–1.45 (m, 2H; CH_2), 0.98 (t, *J*(H,H)=7.4 Hz, 3H; CH_3). ^{13}C NMR (75 MHz, CD_2Cl_2): δ=163.6 (C), 162.0 (C), 145.0 (C), 144.9 (*J*(C,Pt)=77 Hz, C_{trz}–Pt), 144.8 (C), 141.1 (C), 140.4 (CH), 136.0 (*J*(C,Pt)=33 Hz; CH), 129.3 (*J*(C,Pt)=53 Hz; CH), 128.4 (*J*(C,Pt)=15 Hz; CH), 126.2 (*J*(C,Pt)=18 Hz; CH), 125.4 (CH), 124.5 (CH), 116.6 (*J*(C,Pt)=19 Hz; CH), 115.4 (*J*(C,Pt)≈35 Hz; CH), 37.3 (NCH_3), 32.3 (CH_2), 24.2 (CH_2), 23.1 (CH_2), 21.9 (CH_3), 14.2 (CH_3); elemental analysis calcd (%) for $C_{32}H_{31}ClN_4Pt$: C 54.74, H 4.45, N 7.98; found: C 54.58, H 4.49, N, 7.73.

X-ray structure determinations

Single crystals of *trans-C,C**-**3**, *cis-C,C**-**3**, **4**·0.5MeCN, **5**·2CH_2Cl_2, **6** and **7** suitable for X-ray diffraction were obtained by the liquid-liquid diffusion method from CH_2Cl_2/Et_2O (*trans-C,C**-**3**, *cis-C,C**-**3**), CH_2Cl_2/hexane (**5**·2CH_2Cl_2) or CH_3CN/Et_2O (**7**) or by evaporation from an MeCN solution of the complex (**4**·0.5MeCN). The data were collected on a Bruker D8 QUEST diffractometer with monochromated Mo-*K*α radiation performing ω scans (**2**·0.5MeCN) or φ and ω scans (rest of complexes). The structures were solved by direct methods and refined anisotropically on F^2 using the program SHELXL-2018 (G. M. Sheldrick, University of Göttingen).[79] Methyl hydrogens were included as part of rigid idealized methyl groups allowed to rotate but not tip; other hydrogens were included using a riding model. *Special features of refinement:* In *cis-C,C**-**3** and **4**·MeCN, there is a poorly resolved region of residual electron density that could not be adequately modelled and therefore the program SQUEEZE,[80] which is part of the PLATON system, was employed to mathematically remove the effects of the solvent; the void volume per cell was 1033 (*cis-C,C**-**3**) or 228 (**4**·MeCN) Å^3, with a void electron count per cell of 281 (*cis-C,C**-**3**) or 44 (**4**·MeCN); this additional solvent was not taken into account when calculating derived parameters such as the formula weight, because its nature was uncertain. In **5**·2CH_2Cl_2, one of the solvent molecules is disordered over two positions, approximately 58:42%.

CCDC 1893344-1893349 contain the supplementary crystallographic data for this paper. These data can be obtained free of charge from the Cambridge Crystallographic Data Centre via http://www.ccdc.cam.ac.uk/data_request/cif.

Photophysical characterization

UV-vis absorption spectra were recorded on a Perkin-Elmer Lambda 750S spectrophotometer. Excitation and emission spectra were recorded on a Jobin Yvon Fluorolog 3-22 spectrofluorometer with a 450 W xenon lamp, double-grating monochromators, and a TBX-04 photomultiplier. Solution measurements were carried out using 10 mm quartz fluorescence cells (298 K) or 5 mm quartz NMR tubes (77 K). For the low-temperature measurements, a liquid nitrogen Dewar with quartz windows was employed. The photophysical data in PMMA thin films were measured using quartz slides as sample holders. Lifetimes were measured using an IBH FluoroHub controller in MCS mode and the Fluorolog's FL-1040 phosphorimeter pulsed xenon lamp as excitation source; the estimated uncertainty is ±10% or better. Emission quantum yields (Φ) were measured using a Hamamatsu C11347 Absolute PL Quantum Yield Spectrometer; the estimated uncertainty is ±5% or better. Quantum yields lower than 0.01 were determined by the optically dilute method,[81] using [Pt(ppy)$_2$Cl$_2$] (ppy = cyclometalated 2-phenylpyridine) as standard (Φ = 0.114);[23] the estimated uncertainty is ±20%. Luminescence data were obtained under rigorous exclusion of oxygen, by bubbling argon through the solutions or placing the PMMA films under argon.

Computational methods

DFT calculations were carried out with the Gaussian 09 package,[82] using the hybrid B3LYP functional[83,84] together with the 6-31G**[85,86] basis set for the light atoms and the LANL2DZ[87] basis set and effective core potential for the Pt atom. All geometry optimizations were carried out without symmetry restrictions, using "tight" convergence criteria and

"ultrafine" integration grid. Vertical excitation energies were obtained from TDDFT calculations at the ground-state optimized geometries. Triplet state geometry optimizations were carried out following a two-step strategy.[88] Initially, a TDDFT optimization of the target triplet was attempted starting from the ground-state geometry; the resulting geometry was then subjected to a spin-unrestricted DFT (UB3LYP) optimization setting a triplet multiplicity. The solvent effect (CH_2Cl_2) was accounted for in all cases by using the integral equation formalism variant of the polarizable continuum solvation model (IEFPCM).[89] All the optimized structures were confirmed as minima on the potential energy surface by performing frequency calculations (zero imaginary frequencies). Natural spin densities were obtained from natural population analyses using the NBO 5.9 program.[90]

Acknowledgements

We thank the Spanish Ministerio de Economía y Competitividad (CTQ2015-69568-P) and Fundación Séneca (19890/GERM/15) for financial support. Ángela Vivancos thanks Fundación Séneca for a Saavedra Fajardo Fellowship (20398/SF/17).

Keywords: luminescence • NHC ligands • cyclometalating ligands • platinum • carbenes

[1] Y. You, S. Cho, W. Nam, *Inorg. Chem.* **2014**, *53*, 1804–1815.

[2] Y. Yang, Q. Zhao, W. Feng, F. Li, *Chem. Rev.* **2013**, *113*, 192–270.

[3] D.-L. Ma, V. P.-Y. Ma, D. S.-H. Chan, K.-H. Leung, H.-Z. He, C.-H. Leung, *Coord. Chem. Rev.* **2012**, *256*, 3087–3113.

[4] K. K.-W. Lo, *Acc. Chem. Res.* **2015**, *48*, 2985–2995.

[5] D. L. Ma, H. Z. He, K. H. Leung, D. S. H. Chan, C. H. Leung, *Angew. Chem. Int. Ed.* **2013**, *52*, 7666–7682.

[6] E. Baggaley, S. W. Botchway, J. W. Haycock, H. Morris, I. V Sazanovich, J. A. G. Williams, J. A. Weinstein, *Chem. Sci.* **2014**, *5*, 879–886.

[7] Q. Zhao, C. Huang, F. Li, *Chem. Soc. Rev.* **2011**, *40*, 2508–2524.

[8] M. H. Shaw, J. Twilton, D. W. C. MacMillan, *J. Org. Chem.* **2016**, *81*, 6898–6926.

[9] C. K. Prier, D. A. Rankic, D. W. C. MacMillan, *Chem. Rev.* **2013**, *113*, 5322–5363.

[10] R. Lincoln, L. Kohler, S. Monro, H. Yin, M. Stephenson, R. Zong, A. Chouai, C. Dorsey, R. Hennigar, R. P. Thummel, et al., *J. Am. Chem. Soc.* **2013**, *135*, 17161–17175.

[11] S. Monro, K. L. Colón, H. Yin, J. Roque, P. Konda, S. Gujar, R. P. Thummel, L. Lilge, C. G. Cameron, S. A. McFarland, *Chem. Rev.* **2019**, *119*, 797–828.

[12] M. E. Thompson, P. E. Djurovich, S. Barlow, S. Marder, in *Compr. Organomet. Chem. III* (Eds.: H.C. Robert, D.M.P. Mingos), Elsevier, Oxford, **2007**, pp. 101–194.

[13] J. Kalinowski, V. Fattori, M. Cocchi, J. A. G. Williams, *Coord. Chem. Rev.* **2011**, *255*, 2401–2425.

[14] C. Cebrián, M. Mauro, *Beilstein J. Org. Chem.* **2018**, *14*, 1459–1481.

[15] R. D. Costa, E. Ortí, H. J. Bolink, F. Monti, G. Accorsi, N. Armaroli, *Angew. Chem. Int. Ed.* **2012**, *51*, 8178–8211.

[16] L. Flamigni, A. Barbieri, C. Sabatini, B. Ventura, F. Barigelletti, *Top. Curr. Chem.* **2007**, *281*, 143–203.

[17] J. C. Deaton, F. N. Castellano, in *Iridium(III) in Optoelectronic and Photonics Applications* (Ed.: E. Zysman-Colman), John Wiley & Sons, Ltd, Chichester, UK, **2017**, pp. 1–69.

[18] S. Huo, J. Carroll, D. A. K. Vezzu, *Asian J. Org. Chem.* **2015**, *4*, 1210–1245.

[19] A. K. W. Chan, M. Ng, Y. C. Wong, M. Y. Chan, W. T. Wong, V. W. W. Yam, *J. Am. Chem. Soc.* **2017**, *139*, 10750–10761.

[20] R. Kumar, C. Nevado, *Angew. Chem. Int. Ed.* **2017**, *56*, 1994–2015.

[21] C. Bronner, O. S. Wenger, *Dalton Trans.* **2011**, *40*, 12409–12420.

[22] D. M. Jenkins, S. Bernhard, *Inorg. Chem.* **2010**, *49*, 11297–11308.

[23] F. Juliá, M. D. García-Legaz, D. Bautista, P. González-Herrero, *Inorg. Chem.* **2016**, *55*, 7647–7660.

[24] R. R. Parker, J. P. Sarju, A. C. Whitwood, J. A. G. Williams, J. M. Lynam, D. W. Bruce, *Chem. Eur. J.* **2018**, 19010–19023.

[25] F. Juliá, D. Bautista, P. González-Herrero, *Chem. Commun.* **2016**, *52*, 1657–1660.

[26] L. Chassot, A. von Zelewsky, D. Sandrini, M. Maestri, V. Balzani, *J. Am. Chem. Soc.* **1986**, *108*, 6084–6085.

[27] N. Giménez, R. Lara, M. T. Moreno, E. Lalinde, *Chem. Eur. J.* **2017**, *23*, 5758–5771.

[28] F. Juliá, D. Bautista, J. M. Fernández-Hernández, P. González-Herrero, *Chem. Sci.* **2014**, *5*, 1875–1880.

[29] F. Juliá, G. Aullón, D. Bautista, P. González-Herrero, *Chem. Eur. J.* **2014**, *20*, 17346–17359.

[30] F. Juliá, P. González-Herrero, *Dalton Trans.* **2016**, *45*, 10599–10608.

[31] G. S. M. Tong, C. M. Che, *Chem. Eur. J.* **2009**, *15*, 7225–7237.

[32] A. M. Prokhorov, T. Hofbeck, R. Czerwieniec, A. F. Suleymanova, D. N. Kozhevnikov, H. Yersin, *J. Am. Chem. Soc.* **2014**, *136*, 9637–9642.

[33] S. C. F. Kui, F.-F. Hung, S.-L. Lai, M.-Y. Yuen, C.-C. Kwok, K.-H. Low, S. S.-Y. Chui, C.-M. Che, *Chem. Eur. J.* **2012**, *18*, 96–109.

[34] C.-Y. Kuei, S.-H. Liu, P.-T. Chou, G.-H. Lee, Y. Chi, *Dalton Trans.* **2016**, *45*, 15364–15373.

[35] M.-C. Tang, M.-Y. Leung, S.-L. Lai, M. Ng, M.-Y. Chan, V. Wing-Wah Yam, *J. Am. Chem. Soc.* **2018**, *140*, 13115–13124.

[36] C.-H. Lee, M.-C. Tang, W.-L. Cheung, S.-L. Lai, M.-Y. Chan, V. W.-W. Yam, *Chem. Sci.* **2018**, *9*, 6228–6232.

[37] J. Fernandez-Cestau, B. Bertrand, A. Pintus, M. Bochmann, *Organometallics* **2017**, *36*, 3304–3312.

[38] W. P. To, D. Zhou, G. S. M. Tong, G. Cheng, C. Yang, C. M. Che, *Angew. Chem. Int. Ed.* **2017**, *56*, 14036–14041.

[39] C. H. Lee, M. C. Tang, Y. C. Wong, M. Y. Chan, V. W. W. Yam, *J. Am. Chem. Soc.* **2017**, *139*, 10539–10550.

[40] G. Cheng, K. T. Chan, W. P. To, C. M. Che, *Adv. Mater.* **2014**, *26*, 2540–2546.

[41] E. S.-H. Lam, W. H. Lam, V. W.-W. Yam, *Inorg. Chem.* **2015**, *54*, 3624–3630.

[42] Á. Vivancos, C. Segarra, M. Albrecht, *Chem. Rev.* **2018**, *118*, 9493–9586.

[43] K. F. Donnelly, A. Petronilho, M. Albrecht, *Chem. Commun.* **2013**, *49*, 1145–1159.

[44] J. Lee, H.-F. Chen, T. Batagoda, C. Coburn, P. I. Djurovich, M. E. Thompson, S. R. Forrest, *Nat. Mater.* **2016**, *15*, 92–98.

[45] Y. Liu, X. Sun, Y. Si, X. Qu, Y. Wang, Z. Wu, *RSC Adv.* **2014**, *4*, 6284–6292.

[46] F. Monti, M. G. I. La Placa, N. Armaroli, R. Scopelliti, M. Grätzel, M. K. Nazeeruddin, F. Kessler, *Inorg. Chem.* **2015**, *54*, 3031–3042.

[47] B. D. Stringer, L. M. Quan, P. J. Barnard, D. J. D. Wilson, C. F. Hogan, *Organometallics* **2014**, *33*, 4860–4872.

[48] T.-Y. Li, X. Liang, L. Zhou, C. Wu, S. Zhang, X. Liu, G.-Z. Lu, L.-S.

Xue, Y.-X. Zheng, J.-L. Zuo, *Inorg. Chem.* **2015**, *54*, 161–173.

[49] S. Aghazada, A. J. Huckaba, A. Pertegas, A. Babaei, G. Grancini, I. Zimmermann, H. Bolink, M. K. Nazeeruddin, *Eur. J. Inorg. Chem.* **2016**, *2016*, 5089–5097.

[50] V. Adamovich, S. Bajo, P.-L. T. Boudreault, M. A. Esteruelas, A. M. López, J. Martín, M. Oliván, E. Oñate, A. U. Palacios, A. San-Torcuato, et al., *Inorg. Chem.* **2018**, *57*, 10744–10760.

[51] M. A. Esteruelas, A. M. López, E. Onate, A. San-Torcuato, J. Y. Tsai, C. Xia, *Inorg. Chem.* **2018**, *57*, 3720–3730.

[52] C.-F. Chang, Y.-M. Cheng, Y. Chi, Y.-C. Chiu, C.-C. Lin, G.-H. Lee, P.-T. Chou, C.-C. Chen, C.-H. Chang, C.-C. Wu, *Angew. Chem. Int. Ed.* **2008**, *47*, 4542–4545.

[53] S. Fuertes, H. García, M. Perálvarez, W. Hertog, J. Carreras, V. Sicilia, *Chem. Eur. J.* **2015**, *21*, 1620–1631.

[54] Y. Unger, D. Meyer, O. Molt, C. Schildknecht, I. Münster, G. Wagenblast, T. Strassner, *Angew. Chem. Int. Ed.* **2010**, *49*, 10214–10216.

[55] H. Leopold, U. Heinemeyer, G. Wagenblast, I. Münster, T. Strassner, *Chem. Eur. J.* **2017**, *23*, 1118–1128.

[56] A. Tronnier, U. Heinemeyer, S. Metz, G. Wagenblast, I. Muenster, T. Strassner, *J. Mater. Chem. C* **2015**, *3*, 1680–1693.

[57] T. Von Arx, A. Szentkuti, T. N. Zehnder, O. Blacque, K. Venkatesan, *J. Mater. Chem. C* **2017**, *5*, 3765–3769.

[58] J. Soellner, M. Tenne, G. Wagenblast, T. Strassner, *Chem. Eur. J.* **2016**, *22*, 9914–9918.

[59] J. Soellner, T. Strassner, *Chem. Eur. J.* **2018**, *24*, 5584–5590.

[60] Ú. Belío, S. Fuertes, A. Martín, *Dalton Trans.* **2014**, *43*, 10828–10843.

[61] F. Juliá, P. González-Herrero, *J. Am. Chem. Soc.* **2016**, *138*, 5276–5282.

[62] S. Gonell, M. Poyatos, E. Peris, *Dalton Trans.* **2016**, *45*, 5549–5556.

[63] J. Mamtora, S. H. Crosby, C. P. Newman, G. J. Clarkson, J. P. Rourke, *Organometallics* **2008**, *27*, 5559–5565.

[64] P. A. Shaw, J. M. Phillips, C. P. Newman, G. J. Clarkson, J. P. Rourke, *Chem. Commun.* **2015**, *51*, 8365–8368.

[65] P. A. Shaw, G. J. Clarkson, J. P. Rourke, *Organometallics* **2016**, *35*, 3751–3762.

[66] P. A. Shaw, G. J. Clarkson, J. P. Rourke, *Chem. Sci.* **2017**, *8*, 5547–5558.

[67] C. P. Newman, K. Casey-Green, G. J. Clarkson, G. W. V. Cave, W. Errington, J. P. Rourke, *J. Chem. Soc., Dalton Trans.* **2007**, 3170–3182.

[68] J. Brooks, Y. Babayan, S. Lamansky, P. I. Djurovich, I. Tsyba, R. Bau, M. E. Thompson, *Inorg. Chem.* **2002**, *41*, 3055–3066.

[69] A. I. Solomatina, D. V. Krupenya, V. V. Gurzhiy, I. Zlatkin, A. P. Pushkarev, M. N. Bochkarev, N. A. Besley, E. Bichoutskaiad, S. P. Tunik, *Dalton Trans.* **2015**, *44*, 7152–7162.

[70] W. Lu, M. C. W. Chan, K.-K. Cheung, C.-M. Che, *Organometallics* **2001**, *20*, 2477–2486.

[71] V. W. Yam, R. P. Tang, K. M. Wong, X. Lu, *Chem. Eur. J.* **2002**, *8*, 4066–4076.

[72] S. C. F. Kui, S. S.-Y. Chui, C.-M. Che, N. Zhu, *J. Am. Chem. Soc.* **2006**, *128*, 8297–8309.

[73] D.-A. Roşca, D. A. Smith, M. Bochmann, *Chem. Commun.* **2012**, *48*, 7247–7249.

[74] D. A. Smith, D. A. Roşca, M. Bochmann, *Organometallics* **2012**, *31*, 5998–6000.

[75] H. Na, P. N. Lai, L. M. Cañada, T. S. Teets, *Organometallics* **2018**, *37*, 3269–3277.

[76] A. F. Rausch, L. Murphy, J. A. G. Williams, H. Yersin, *Inorg. Chem.* **2012**, *51*, 312–319.

[77] D. C. Powers, D. Benitez, E. Tkatchouk, W. A. Goddard, T. Ritter, *J. Am. Chem. Soc.* **2010**, *132*, 14092–14103.

[78] A. Poulain, D. Canseco-Gonzalez, R. Hynes-Roche, H. Müller-Bunz, O. Schuster, H. Stoeckli-Evans, A. Neels, M. Albrecht, *Organometallics* **2011**, *30*, 1021–1029.

[79] G. M. Sheldrick, *Acta Crystallogr., Sect. A Found. Crystallogr.* **2008**, *64*, 112–122.

[80] A. L. Spek, *Acta Crystallogr. Sect. C Struct. Chem.* **2015**, *71*, 9–18.

[81] J. N. Demas, G. A. Crosby, *J. Phys. Chem.* **1971**, *75*, 991–1024.

[82] Gaussian 09, Revision A.02, M. J. Frisch, G. W. Trucks, H. B. Schlegel, G. E. Scuseria, M. A. Robb, J. R. Cheeseman, G. Scalmani, V. Barone, B. Mennucci, G. A. Petersson, H. Nakatsuji, M. Caricato, X. Li, H. P. Hratchian, A. F. Izmaylov, J. Bloino, G. Zheng, J. L. Sonnenberg, M. Hada, M. Ehara, K. Toyota, R. Fukuda, J. Hasegawa, M. Ishida, T. Nakajima, Y. Honda, O. Kitao, H. Nakai, T. Vreven, J. A. Montgomery, Jr., J. E. Peralta, F. Ogliaro, M. Bearpark, J. J. Heyd, E. Brothers, K. N. Kudin, V. N. Staroverov, R. Kobayashi, J. Normand, K. Raghavachari, A. Rendell, J. C. Burant, S. S. Iyengar, J. Tomasi, M. Cossi, N. Rega, N. J. Millam, M. Klene, J. E. Knox, J. B. Cross, V. Bakken, C. Adamo, J. Jaramillo, R. Gomperts, R. E. Stratmann, O. Yazyev, A. J. Austin, R. Cammi, C. Pomelli, J. W. Ochterski, R. L. Martin, K. Morokuma, V. G. Zakrzewski, G. A. Voth, P. Salvador, J. J. Dannenberg, S. Dapprich, A. D. Daniels, Ö. Farkas, J. B. Foresman, J. V. Ortiz, J. Cioslowski, D. J. Fox, Gaussian Inc., Wallingford CT, 2009.

[83] A. Becke, *J. Chem. Phys.* **1993**, *98*, 5648–5652.

[84] C. T. Lee, W. T. Yang, R. G. Parr, *Phys. Rev. B* **1988**, *37*, 785–789.

[85] P. C. Hariharan, J. A. Pople, *Theor. Chim. Acta* **1973**, *28*, 213–222.

[86] M. M. Francl, W. J. Pietro, W. J. Hehre, J. S. Binkley, M. S. Gordon, D. J. Defrees, J. A. Pople, *J. Chem. Phys.* **1982**, *77*, 3654–3665.

[87] P. J. Hay, W. R. Wadt, *J. Chem. Phys.* **1985**, *82*, 299–310.

[88] D. Escudero, W. Thiel, *Inorg. Chem.* **2014**, *53*, 11015–11019.

[89] J. Tomasi, B. Mennucci, R. Cammi, *Chem. Rev.* **2005**, *105*, 2999–3093.

[90] NBO 5.9, E. D. Glendening, J. K. Badenhoop, A. E. Reed, J. E. Carpenter, J. A. Bohmann, C. M. Morales, F. Weinhold, **2009**.

Entry for the Table of Contents

FULL PAPER

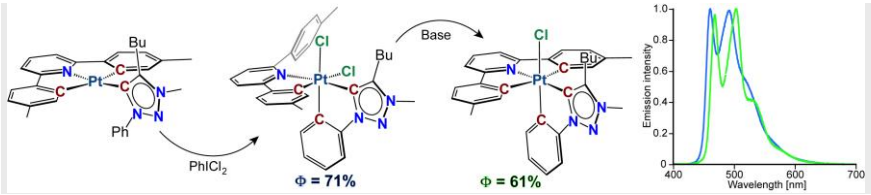

The cyclometalation of an aryl-NHC ligand on the coordination sphere of Pt^{IV} has been achieved for the first time by employing a Pt^{II} precursor with a terdentate C^N^C ligand. Photophysical and computational data provide insight into the effects of the carbene on the luminescence of the resulting complexes.

*Ángela Vivancos, Delia Bautista and Pablo González-Herrero**

Page No. – Page No.

Luminescent platinum(IV) complexes bearing cyclometalated 1,2,3-triazolylidene and bi- or terdentate 2,6-diarylpyridine ligands